Table 4. Myxofibrosarcoma with multiple malignancies (n = 13)

Patient	Age (years)	Gender	FT	Site	CT	RT	MFSP	SPT	Site	CT	RT	MFSP from SPT	TPT	Site	CT	RT	MFSP from TPT	FPT	Site	CT	RT	Prognosis	OS
1	55	Male	MFS	Thigh	–	–	4	Ad	Stomach	–	–	–	–	–	–	–	–	–	–	–	–	NED	10
2	68	Male	MFS	Buttock	–	–	8	Sq	Pharynx	–	50 Gy	–	–	–	–	–	–	–	–	–	–	DOD	246
3	48	Female	MFS	Leg	–	–	130	Ad	Ovary	CDDP + ADR + CPA CDDP + Taxel	–	–	–	–	–	–	–	–	–	–	–	DOD	177
4	69	Male	Ad	Stomach	–	–	38	MFS	Thigh	–	–	–	–	–	–	–	–	–	–	–	–	DOD	101
5	66	Male	TCC	Bladder	–	–	11	MFS	Chest wall	–	–	5	TCC	Bladder	ADR	–	–	–	–	–	–	NED	156
6	69	Male	Sq	tongue	CDDP 5FU	50 Gy	84	MFS	Leg	–	–	7	Sq	Gingiva	–	–	–	–	–	–	–	NED	91
7	70	Male	Ad	Rectum	–	–	19	MFS	Arm	–	42 Gy	–	–	–	–	–	–	–	–	–	–	DOD	34
8	74	Male	Ad	Prostate	–	–	4	MFS	Arm	–	–	–	–	–	–	–	–	–	–	–	–	NED	24
9	48	Female	Ad	Breast	–	–	85	MFS	Arm	–	–	–	–	–	–	–	–	–	–	–	–	NED	143
10	79	Female	RCC	Kidney	–	–	139	MFS	Arm	–	–	–	–	–	–	–	–	–	–	–	–	NED	148
11	77	Male	Ad	Colon*	–	–	275	Ad	Stomach	–	–	105	MFS	Leg	–	–	–	–	–	–	–	NED	381
12	45	Male	Ad	Stomach	–	–	216	Sq	Esophagus	–	60 Gy	84	MFS	Thigh	–	–	–	–	–	–	–	NED	408
13	62	Male	Ad	Colon	–	–	69	Ad	Cecum	–	–	142	Ad	Colon	–	–	120	MFS	Thigh	CDDP	–	NED	331

FT, first tumor; CT, chemotherapy; RT, radiotherapy; MFSP, malignancy-free survival period (months); SPT, second primary tumor; TPT, third primary tumor; FPT, fourth primary tumor; DOD, died of disease; NED, no evidence of disease; OS, overall survival (months); MFS, myxofibrosarcoma; Ad, adenocarcinoma; Sq, squamous cell carcioma; TCC, transitional cell carcinoma; RCC, renal cell carcinoma; CDDP, cisplatin; ADR, adriamycin; CPA, cyclophosphamide; 5FU, 5-fluorouracil.
*Synchronous tumor.

and the second malignancy ranged from 1 to 141 months (median: 60.0 months). The 5- and 10-year estimated cumulative incidence of multiple malignancies in this group was 5.1% (95% CI 2.2–8.0) and 9.7% (95% CI 3.8–15.7%; Fig. 1), respectively. The overall survival time of the 16 patients from the time of diagnosis of the first tumor ranged from 6 to 223 months (median: 96.5 months). No significant difference in 5-year survival rate was found between the patients with and without multiple malignancies (66.1 versus 71.6%, $P = 0.80$).

DISCUSSION

The objective of this study was to review the incidence of multiple malignancy in adult STS patients. The results of the analysis showed that 9% of the patients had multiple malignancies. The 5- and 10-year estimated cumulative incidence of multiple malignancy was 7.6% (95% CI 4.7–10.4) and 12.3% (95% CI 7.4–18.0), respectively. In addition, the risk of multiple malignancy appeared to be impacted by age at the time of diagnosis of the first tumor and by the histological type of myxofibrosarcoma.

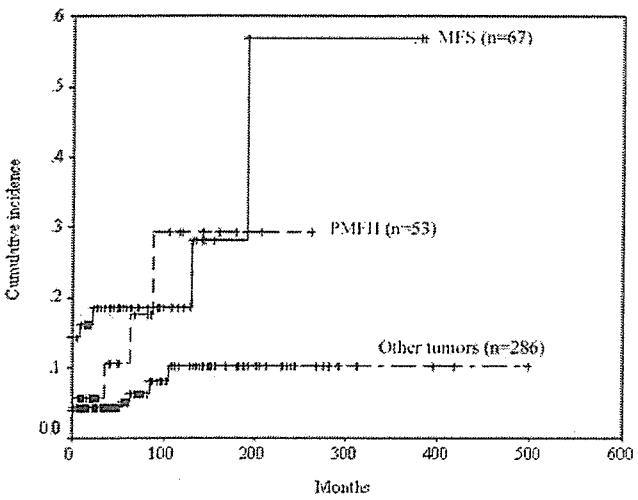

Figure 1. Cumulative incidence of multiple malignancies in STS. MFS, myxofibrosarcoma; PMFH, pleomorphic malignant fibrous histiocytoma. A statistically significant difference is found between the three groups (log rank $P = 0.002$).

The results of this analysis add to the evidence of an association between STS and the risk of multiple malignancy. The results are consistent with the findings in the cohort study Merimsky et al. that assessed the risk of multiple malignancies associated with STS (11). In their study, 28 of 375 adult patients (7.5%) with STS were found to have developed another primary malignant neoplasm either before or after the diagnosis of STS, a significantly higher rate than reported for the occurrence of STS in the general cancer patient population (1.0%). In addition, they also observed an association between primary MFH and the occurrence of renal cell carcinoma. However, Merimsky et al. did not evaluate risk according to histological types of STS, and they included several patients with bone sarcoma in their analysis. Thus, our study expanded on the findings of Merimsky et al. by assessing the impact of histological type.

Previous studies in patients with STS have found frequencies of an SPT ranging from 1.2 to 6.0% (14,15). In contrast, one study that investigated the risk of developing SPT in patients with non-Hodgkin lymphoma yielded a frequency of 15.4% (16). However, the populations in these studies were mainly children or adolescents. In our study, the rate of association of an SPT or TPT with STS was 9.0%, suggesting that the frequency of multiple malignancies is similar in the different age populations. Age at the time of diagnosis was strongly associated with increased risk of multiple malignancies in adult patients with STS.

The results of our study showed that the risk of multiple malignancies was similar when the analysis was conducted separately for patients with pleomorphic MFH and myxofibrosarcoma, the most common types of STS. Multiple malignancies were detected in six patients with pleomorphic MFH, and in five patients where the pleomorphic MFH was preceded by another malignant tumor. Similarly, the other malignancy was detected first in three of the 13 patients (23%) with myxofibrosarcoma and subsequently in the other

Table 5. Pleomorphic MFH with multiple malignancies ($n = 6$)

Patient	Age (years)	Gender	FT	Site	CT	RT	MFSP	SPT	Site	CT	RT	MFSP from SPT	TPT	Site	CT	RT	Prognosis	OS
1	76	Male	PMFH	Shoulder	–	32.5 Gy	64	Ad	Bile duct	MMC	–	–	–	–	–	–	DOD	78
2	76	Male	PMFH	Thigh	–	–	84	Ad	Lung	–	–	–	–	–	–	–	DOD	155
3	53	Male	PMFH	Elbow	VCR ADR	–	6	Sq	Tongue	–	–	–	–	–	–	–	DOD	106
4	47	Male	PMFH	Buttock	–	–	31	Ad	Colon	–	–	–	–	–	–	–	DOD	48
5	76	Male	PMFH	Back	–	50 Gy	121	Ad	Stomach	–	50 Gy	–	–	–	–	–	DOD	138
6	71	Male	Sq	Esophagus	–	–	94	PMFH	Back	–	–	7	Ad	Stomach	–	–	DOD	120

FT, first tumor; CT, chemotherapy; RT, radiotherapy; MFSP, malignancy-free survival period (months); SPT, second primary tumor; TPT, third primary tumor; DOD, died of disease; NED, no evidence of disease; OS, overall survival (months); PMFH, pleomorphic malignant fibrous histiocytoma; Sq, squamous cell carcioma; Ad, adenocarcinoma; VCR, vincristine; ADR, adriamycin; MMC, mitomycin C.

Table 6. Other tumors with multiple malignancies (n = 16)

Patient	Age (years)	Gender	FT	Site	CT	RT	MFSP	SPT	Site	CT	RT	MFSP from SPT	TPT	Site	CT	RT	Prognosis	OS
1	62	Female	FS	Thigh	–	–	1	Ad	Uterine	–	–	–	–	–	–	–	DOD	6
2	57	Female	LS (D)	Retroperitoneum	–	40 Gy	29	Ad	Breast	–	–	–	–	–	–	–	DOD	108
3	42	Female	LS (D)	Retroperitoneum	ADR VCR	–	75	Pap	Thyroid	NA	NA	–	–	–	–	–	DOD	78
4	57	Male	LS (M)	Thigh	VCR	–	141	Sq	Larynx	–	60 Gy	–	–	–	–	–	NED	223
5	59	Male	LS (M)	Thigh	–	–	4	Ad	Lung*	–	–	–	–	–	–	–	NED	38
6	61	Male	LS (WD)	Retroperitoneum	–	–	81	Ad	Prostate	SR	62 Gy	–	–	–	–	–	NED	85
7	63	Male	LS (WD)	Retroperitoneum	–	–	8	Ad	Prostate	LA	–	–	–	–	–	–	NED	9
8	70	Female	Ad	Breast	–	–	60	FS	Chest wall	–	–	17	Ad	Stomach	–	–	NED	112
9	60	Male	DLBL	Thyroid	CHOP	–	81	L	Leg	–	–	–	–	–	–	–	NED	117
10	39	Female	Ad	Breast	–	–	60	L	Buttock	CPA, VCR, ADM, DTIC	–	–	–	–	–	–	DOD	212
11	50	Female	Ad	Breast	–	–	105	LS (M)	Thigh	–	50 Gy	–	–	–	–	–	DOD	127
12	64	Male	Ad	Rectum	–	–	50	LS (M)	Leg	–	–	–	–	–	–	–	DOD	61
13	43	Female	Ad	Breast	–	–	102	LS (WD)	Retroperitoneum	–	–	–	–	–	–	–	NED	121
14	63	Female	Ad	Breast	–	–	29	LS (WD)	Retroperitoneum	–	–	–	–	–	–	–	NED	75
15	71	Female	Pap	Thyroid	–	–	2	MPNST	Retroperitoneum	–	–	–	–	–	–	–	NED	15
16	79	Male	TCC	Bladder	–	–	106	Ad	Lung	–	–	12	LS (D)	Retroperitoneum	–	–	DOD	146

FT, first tumor; CT, chemotherapy; RT, radiotherapy; MFSP, malignancy-free survival period (months); SPT, second primary tumor; TPT, third primary tumor; DOD, died of disease; NED, no evidence of disease; OS, overall survival (months); FS, fibrosarcoma; Ad, adenocarcinoma; LS (D), liposarcoma (dedifferentiated); Pap, papillary carcinoma; LS (M), liposarcoma (myxoid); Sq, squamous cell carcinoma; LS (WD), liposarcoma (well differentiated); DLBL, diffuse large B-cell lymphoma; MPNST, malignant peripheral nerve sheath tumor; TCC, transitional cell carcinoma; CHOP, cyclophosphamide, adriamycin, vincristine, prednisolone; ADR, adriamycin; VCR, vincristine; CPA, cyclophosphamide; DTIC, dacarbazine; SR, zoladex; LA, leuplin; NA, not applicable.
*Synchronous tumor.

10 patients (77%). Some investigators consider a pleomorphic MFH to be a high grade tumor that has a substantially high metastatic rate and poor prognosis (17,18). Myxofibrosarcoma is a distinct fibroblastic neoplasm that may recur and has a relatively poor prognosis (19–21). In our study, univariate analysis revealed that no significant association was found between risk of multiple malignancy and survival rate, or familiar history in pleomorphic MFH and myxofibrosarcoma.

A family history of cancer and genetic predisposition to cancer may be associated with a risk of multiple malignancies. A correlation between the incidence of multiple malignancy and familial aggregation has been demonstrated in Li–Fraumeni syndrome (22). Similarly, genetic factors have an impact on the risk of various histological types of SPT (23,24). It was not likely that these factors would profoundly influence the risk related to development of multiple malignancies since there was no significant association between familial history of cancer and the risk of multiple malignancies in our study. Some rare familial syndromes are associated with an excess risk of multiple malignancies. There was a patient with FAP with a germline mutation of the APC gene. This patient developed myxofibrosarcoma of the thigh as a fourth primary tumor after surgical treatment of colon cancers three times.

Despite the fact that the known carcinogenic effects of chemotherapy and radiation therapy are associated with an increased risk of developing SPT (25,26), no interaction was found with having received chemotherapy and radiation therapy according to the results of the multivariate analysis. The lack of agreement between our findings and those of other investigators may be attributable to the small number of patients treated by chemotherapy and radiation therapy: only two patients with second or third primary STS were previously treated by chemotherapy and radiation therapy.

Our results showed that multiple malignancies occurred in 9% of patients with STS, and that the rate of occurrence depended on the histological type. The 5-year survival rate of patients with multiple malignancies according to the histological type of STS was not statistically different from that of the patients without multiple malignancies. Many histological types of multiple malignancies occurred in various organs, suggesting that the whole-body screening to detect other primary malignant neoplasms in addition to local recurrence or distant metastasis should be considered in the management of patients with multiple primary malignancies. Recent prospective studies have highlighted the potential diagnostic role of whole-body [^{18}F]fluorodeoxyglucose positron emission tomography (FDG PET) for evaluation of malignant tumors. FDG PET is an accurate non-invasive test for diagnosis of adult STS and has high sensitivity and intermediate specificity for malignancy. We recommend a whole-body FDG PET scan in the search for a second malignancy in patients with multiple primary malignancies.

In summary, the results of our study confirm the incidence of multiple primary malignancies in adult patients with STS, and the histological type of myxofibrosarcoma was found to be associated with an increased risk of multiple primary malignancy. Physicians should be aware of the increased risk of multiple primary malignancies in patients with myxofibrosarcoma, and whole-body screening to detect other malignant neoplasms is desirable.

References

1. Evans HS, Lewis CM, Robinson D, Bell CMJ, Høller H, Hodgson SV. Incidence of multiple primary cancers in a cohort of women diagnosed with breast cancer in southeast England. *Br J Cancer* 2001;84:435–40.
2. Rubino C, de Vathaire F, Dottorini ME, Hall P, Schvartz C, Couette JE, et al. Second primary malignancies in thyroid cancer patients. *Br J Cancer* 2003;89:1638–44.
3. Leung W, Sandlund JT, Hudson MM, Zhou Y, Hancock ML, Zhu Y, et al. Second malignancy after treatment of childhood non-Hodgkin lymphoma. *Cancer* 2001;92:1959–66.
4. Hasegawa T, Matsuno Y, Niki T, Hirohashi S, Shimoda T, Takayama J, et al. Second primary rhabdomyosarcomas in patients with bilateral retinoblastoma: a clinicopathologic and immunohistochemical study. *Am J Surg Pathol* 1998;22:1351–60.
5. Bokemeyer C, Schmoll HJ. Secondary neoplasms following treatment of malignant germ cell tumors. *J Clin Oncol* 1993;11:1703–9.
6. Hartmann JT, Nichols CR, Droz JP, Horwich A, Gerl A, Fossa SD, et al. The relative risk of second nongerminal malignancies in patients with extragonadal germ cell tumors. *Cancer* 2000;88:2629–35.
7. Heyn R, Haeberlen V, Newton WA, Ragab AH, Raney RB, Tefft M, et al. Second malignant neoplasms in children treated for rhabdomyosarcoma. Intergroup Rhabdomyosarcoma Study Committee. *J Clin Oncol* 1993;11:262–70.
8. Scaradavou A, Heller G, Sklar CA, Ren L, Ghavimi F. Second malignant neoplasms in long-term survivors of childhood rhabdomyosarcoma. *Cancer* 1995;76:1860–7.
9. Pratt CB, Meyer WH, Luo X, Cain AM, Kaste SC, Pappo AS, et al. Second malignant neoplasms occurring in survivors of osteosarcoma. *Cancer* 1997;80:960–5.
10. Aung L, Gorlick RG, Shi W, Thaler H, Shorter NA, Healey JH, et al. Second malignant neoplasms in long-term survivors of osteosarcoma: Memorial Sloan-Kettering Cancer Center Experience. *Cancer* 2002;95:1728–34.
11. Merimsky O, Kollender Y, Issakov J, Bickels J, Flusser G, Gutman M, et al. Multiple primary malignancies in association with soft tissue sarcomas. *Cancer* 2001;91:1363–71.
12. Fletcher CDM, Unni KK, Mertens F, eds. World Health Organization Classification of Tumours. Pathology and Genetics of Tumours of Soft Tissue and Bone. Lyon, France: IARC Press;2002.
13. Hasegawa T, Yamamoto S, Yokoyama R, Umeda T, Matsuno Y, Hirohashi S. Prognostic significance of grading and staging systems using MIB-1 score in adult patients with soft tissue sarcoma of the extremities and trunk. *Cancer* 2002;95:843–51.
14. Kuttesch JF Jr, Wexler LH, Marcus RB, Fairclough D, Weaver-McClure L, White M, et al. Second malignancies after Ewing's sarcoma: radiation dose-dependency of secondary sarcomas. *J Clin Oncol* 1996;14:2818–25.
15. Rich DC, Corpron CA, Smith MB, Black CT, Lally KP, Andrassy RJ. Second malignant neoplasms in children after treatment of soft tissue sarcoma. *J Pediatr Surg* 1997;32:369–372.
16. Green DM, Hyland A, Barcos MP, Reynolds JA, Lee RJ, Hall BC, et al. Second malignant neoplasms after treatment for Hodgkin's disease in childhood or adolescence. *J Clin Oncol* 2000;18:1492–9.
17. Fletcher CD, Gustafson P, Rydholm A, Willen H, Akerman M. Clinicopathologic re-evaluation of 100 malignant fibrous histiocytomas: prognostic relevance of subclassification. *J Clin Oncol* 2001;19:3045–50.
18. Coindre JM, Terrier P, Guillou L, Le Doussal V, Collin F, Ranchere D, et al. Predictive value of grade for metastasis development in the main histologic types of adult soft tissue sarcomas: a study of 1240 patients from the French Federation of Cancer Centers Sarcoma Group. *Cancer* 2001;91:1914–26.
19. Mentzel T, Calonje E, Wadden C, Camplejohn RS, Beham A, Smith MA, et al. Myxofibrosarcoma. Clinicopathologic analysis of 75 cases with emphasis on the low-grade variant. *Am J Surg Pathol* 1996;20:391–405.
20. Weiss SW, Goldblum JR (2001) Fibrosarcoma. In: Enzinger and Weiss's Soft Tissue Tumours, 4th edn. St Louis: Mosby; 2001:423–5.

21. Huang HY, Lal P, Qin J, Brennan MF, Antonescu CR. Low-grade myxofibrosarcoma: a clinicopathologic analysis of 9 cases treated at a single institution with simultaneous assessment of the efficacy of 3-tier and 4-tier grading systems. *Hum Pathol* 2004;35:612–21.
22. Li FP, Fraumeni JF Jr. Prospective study of a family cancer syndrome. *J Am Med Assoc* 1982;247:2692–4.
23. Malkin D, Jolly KW, Barbier N, Look AT, Friend SH, Gebhardt MC, et al. Germline mutations of the p53 tumor-suppressor gene in children and young adults with second malignant neoplasms. *N Engl J Med* 1992;326:1309–15.
24. Kony SJ, de Vathaire F, Chompret A, Shamsaldim A, Grimaud E, Raquin MA, et al. Radiation and genetic factors in the risk of second malignant neoplasms after a first cancer in childhood. *Lancet* 1997; 350:91–5.
25. Chaplain G, Milan C, Sgro C, Carli PM, Bonithon-Kopp C. Increased risk of acute leukemia after adjuvant chemotherapy for breast cancer: a population-based study. *J Clin Oncol* 2000;18:2836–42.
26. Huang J, Mackillop WJ. Increased risk of soft tissue sarcoma after radiotherapy in women with breast carcinoma. *Cancer* 2001;92:172–80.

Ukihide Tateishi[1]
Tadashi Hasegawa[2]
Hiroaki Onaya[1]
Mitsuo Satake[1]
Yasuaki Arai[1]
Noriyuki Moriyama[1]

Myxoinflammatory Fibroblastic Sarcoma: MR Appearance and Pathologic Correlation

OBJECTIVE. The purpose of our study was to define the MR appearance of myxoinflammatory fibroblastic sarcoma of the soft tissues and to make correlations with the histopathologic features.

CONCLUSION. Myxoinflammatory fibroblastic sarcoma is an uncommon malignancy that typically affects adult subjects, who present with painless swelling. This lesion manifests on MR images as a poorly circumscribed mass involving the underlying tendon sheath in the distal extremities.

Myxoinflammatory fibroblastic sarcoma of the soft tissues is a rare low-grade tumor of uncertain origin that usually arises in the hands and feet. Myxoinflammatory fibroblastic sarcoma was first described in 1998 by Meis-Kindblom and Kindblom [1]. Montgomery et al. [2] named the tumor "inflammatory myxohyaline tumor" of the distal extremities with virocyte or Reed-Sternberg-like cells. Histologic characteristics are the spindle to epithelioid neoplastic cells as the manifestation of malignancy admixed with the myxoid and hyalinized matrix, the inflammatory infiltrate, and bizarre virocyte or Reed-Sternberg-like cells with enlarged vesicular nuclei [1–3].

More than 100 cases of myxoinflammatory fibroblastic sarcoma have been reported, with a large series identified in two articles [1–6]. However, MRI findings of myxoinflammatory fibroblastic sarcoma have rarely been documented. The purpose of this study was to characterize the MR appearance of myxoinflammatory fibroblastic sarcoma and to correlate that appearance with the histopathologic features.

Materials and Methods

MR images of all patients with pathologically proven myxoinflammatory fibroblastic sarcoma at our institution were retrospectively reviewed. Our institutional review board gave its approval for a review of patient records and images. The patients were identified by review of our institution's pathology database for a 2-year period. The affected patients included three males and one female who ranged in age from 15 to 62 years old (mean age, 35 years). All histopathologic specimens were reviewed by an experienced pathologist to confirm the diagnosis. Histopathologic examination in all patients showed spindle and epithelioid tumor cells with mild nuclear atypia. Ganglionlike cells and Reed-Sternberg-like cells were also prominent in all cases. Inflammatory cells, including neutrophils, lymphocytes, and eosinophils, were densely present in all cases. Immunohistochemistry was performed in all patients, and all tumors displayed immunoreactivity to vimentin, smooth-muscle actin, and CD34. These histopathologic characteristics were compatible with the diagnosis of myxoinflammatory fibroblastic sarcoma [7]. Medical records were reviewed by one of the authors for presenting complaints, disease progression, and outcome. Radiographs, available for all patients, were also evaluated by two radiologists for the presence of soft-tissue masses or nodules, mineralization, and bone destruction. The findings were recorded by consensus.

T1- and T2-weighted MR images were obtained in the sagittal and coronal planes using a surface coil. T1-weighted conventional spin-echo MR images were obtained using a 20-cm field of view, 3.5- to 5-mm section thickness, TR range/TE of 450–520/15, 160 × 256 matrix, and 2 signals acquired. T2-weighted fast spin-echo acquisitions with ($n = 3$) or without ($n = 1$) fat suppression were performed using a 20-cm field of view, 3.5- to 5-mm section thickness, 3,600–4,000/120, 160 × 256 ma-

Received June 2, 2004; accepted after revision July 28, 2004.

Supported in part by grant for Scientific Research Expenses for Health and Welfare Programs, The Foundation for the Promotion of Cancer Research, and second-term Comprehensive 10-year Strategy for Cancer Control.

[1]Division of Diagnostic Radiology, National Cancer Center Hospital and Institute, Tsukiji, Chuo-Ku, 104-0045, Tokyo, Japan. Address correspondence to U. Tateishi.

[2]Pathology Division, National Cancer Center Hospital and Institute, Tsukiji, Tokyo, Japan.

AJR 2005;184:1749–1753

0361–803X/05/1846–1749

trix, and 2 signals acquired. After the IV administration of 0.1 mmol of gadopentetate dimeglumine (Magnevist, Schering) per kilogram of body weight, transverse T1-weighted images with ($n = 3$) or without ($n = 1$) fat suppression were obtained in the sagittal and coronal planes.

MR images were reviewed by two radiologists and findings were recorded by consensus. Images were evaluated for lesion location and size, depth (superficial or deep), shape of margin (well or ill defined), and the presence or absence of extracompartmental extension. To define depth, superficial lesions did not involve the superficial fascia, and deep lesions were deep in relation to or invaded the superficial fascia. The relationship between tumor and the underlying tendon sheath was also evaluated. MR images were evaluated for predominant signal intensity characteristics (low, intermediate, high), signal homogeneity or heterogeneity, and enhancement characteristics. On T1-weighted images, low signal intensity was defined as signal intensity less than that of muscle; intermediate signal intensity, similar to that of muscle; and high signal intensity, similar to that of fat. On T2-weighted images, low signal intensity was defined as signal intensity similar to that of muscle; intermediate signal intensity, greater than that of muscle but less than that of fat; and high signal intensity, equal to or greater than that of fat. Tumor enhancement was visually graded as greater than, less than, or equal to that of surrounding muscle and vessels.

Results

Clinical Features

All patients were symptomatic at presentation. Presenting complaints were painless swelling of the distal extremities. The mean symptom duration was 4.8 months. Tumors arose from the feet ($n = 2$), hands ($n = 1$), and fingers ($n = 1$). All patients received excisional biopsy for definitive diagnosis and primary therapy. Surgical margins were adequate in three patients and inadequate in one patient. The one patient with an inadequate surgical margin underwent subsequent wide resection. Chemotherapy and radiation therapy were not included in the treatment regimen in any patient. Local recurrence occurred 26.5 months after the initial surgery in two patients. These patients received wide resection. At the latest follow-up (27–82 months; mean, 45 months), no patients had developed further recurrence or metastasis.

MRI Findings and Pathologic Correlations

The gross characteristics of the resected specimens featured multinodular architecture corresponding to MRI features. The mean tumor diameter was 2.4 cm (range, 1.2–3.0 cm). Tumors were located along the tendon sheath in all patients. Findings of extensive involvement surrounding the tendon sheath by the tumor were seen. In two patients, the tumor existed beneath the tendon sheath (Fig. 1), and in two it involved the surrounding tendon sheath diffusely and focally infiltrated the dermis (Fig. 2). One patient had an ill-defined, irregularly marginated mass involving the ulnar nerve and the tendon sheath of the flexor carpi ulnaris (Fig. 2).

Cortical invasion was not identified in any patient on radiographs. All tumors showed predominantly low signal intensity relative to muscle on T1-weighted MR images (Fig. 3). Two lesions showed moderate and homogeneous enhancement after the IV administration of contrast material (Figs. 1 and 3). The cut surface of resected specimens showed solid nests of neoplastic cells that featured spindle and epithelioid cells with higher cellularity, which corresponded to homogeneous enhancement on contrast-enhanced MR images. Two lesions showed heterogeneous enhancement of the tumor that correlated with geographic areas of the myxoid stromal matrix on microscopic observations (Fig. 4). On T2-weighted MR images, all lesions had intermediate signal intensity greater than that of muscle but less than that of fat (Fig. 2). In all cases, the cut surface of specimens revealed solid nests of cellular areas with foci of hyalinized collagen fibers and hypocellular areas with a myxoid stromal

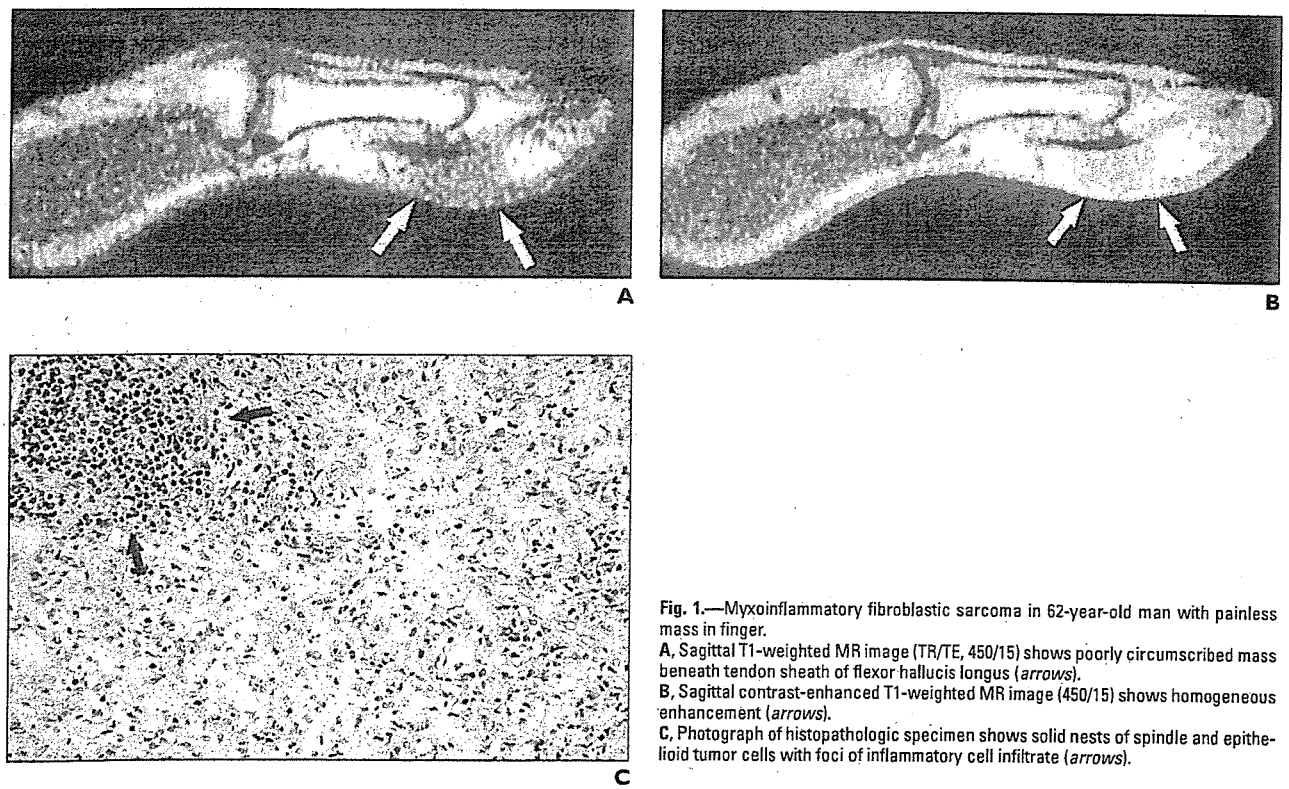

Fig. 1.—Myxoinflammatory fibroblastic sarcoma in 62-year-old man with painless mass in finger.
A, Sagittal T1-weighted MR image (TR/TE, 450/15) shows poorly circumscribed mass beneath tendon sheath of flexor hallucis longus (*arrows*).
B, Sagittal contrast-enhanced T1-weighted MR image (450/15) shows homogeneous enhancement (*arrows*).
C, Photograph of histopathologic specimen shows solid nests of spindle and epithelioid tumor cells with foci of inflammatory cell infiltrate (*arrows*).

matrix, which corresponded to the imaging appearance of intermediate signal intensity on T2-weighted MR images.

Two patients developed recurrent tumors and underwent follow-up MRI after treatment. One patient developed a mass of sheetlike appearance beneath the dorsal portion of the underlying tendon sheath (Fig. 3). Signal characteristics and homogeneous enhancement patterns were similar to those of the primary tumors. Histopathologic examination of this patient showed an infiltrate of lymphoid cells and a marked proliferation of spindle-shaped tumor cells surrounding the tendon sheaths.

In the second patient, a mass of branching pattern occurred along the extensor digitorum longus tendon sheaths of the second and fourth toes without distortion of the architecture of the tendon sheaths (Fig. 4). This patient had also MRI findings suggesting capsular involvement in the metatarsophalangeal joint of the second toe. Histopathologic examination revealed that the tumor arose from the extensor digitorum longus tendon sheaths and also involved the extensor digitorum brevis tendon sheath, cutaneous nerve, and dermis.

Discussion

Myxoinflammatory fibroblastic sarcoma is a rare tumor of the subcutaneous soft tissue that can arise on the trunk but most commonly occurs in the distant extremities [1, 2]. According to the literature and our experience, myxoinflammatory fibroblastic sarcoma is a tumor that most commonly affects adults who are symptomatic at presentation [1, 2]. All patients in our series were symptomatic, with common complaints of a painless mass.

Myxoinflammatory fibroblastic sarcoma has a relatively good prognosis with a long life expectancy despite frequent local recurrence [1–3]. Two of our patients developed local recurrence, with an average duration of 26.5 months. According to the literature, the local recurrence rate in patients with myxoinflammatory fibroblastic sarcoma ranges from 22% to 67% [1, 2]. The metastasis rate in patients with myxoinflammatory fibroblastic sarcoma is uncertain. Metastases have been reported to develop in only a few cases [1].

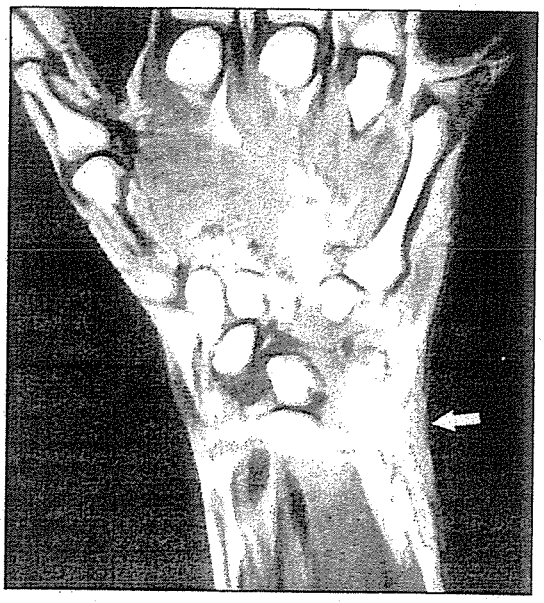

A

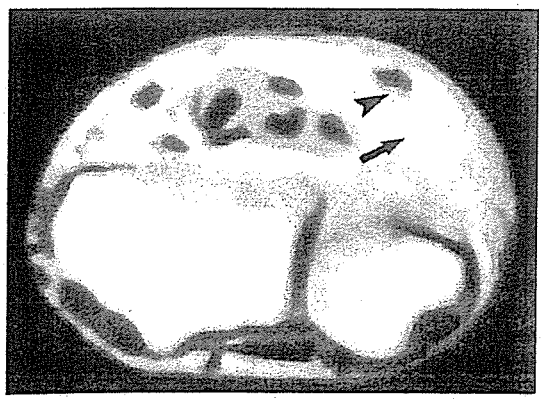

B

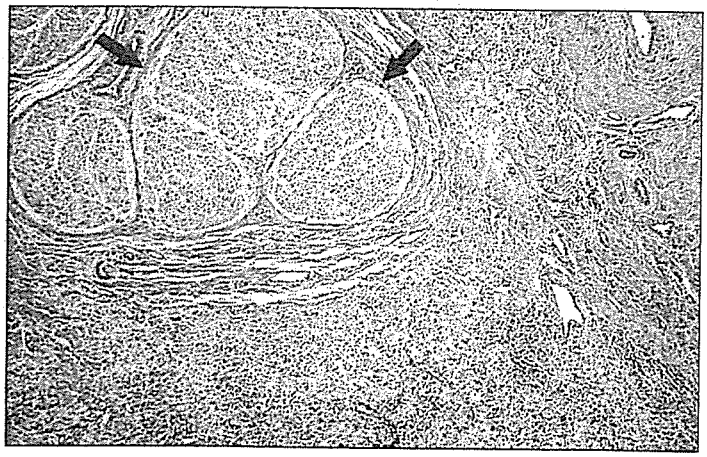

C

Fig. 2.—Myxoinflammatory fibroblastic sarcoma in 31-year-old man with painless mass in subcutaneous soft tissue of wrist.
A, Coronal contrast-enhanced T1-weighted MR image (TR/TE, 520/15) shows poorly circumscribed mass with ill-defined border. Tumor involves surrounding tendon sheath diffusely and focally infiltrates dermis (*arrow*).
B, Axial contrast-enhanced T1-weighted MR image (520/15) shows mass involving ulnar nerve (*arrow*) and tendon sheath of flexor carpi ulnaris (*arrowhead*).
C, Photograph of histopathologic specimen reveals that numerous small nodules consisting of tumor cells infiltrate along ulnar nerve (*arrows*).

In all of our patients, excisional biopsy for definitive diagnosis and primary therapy was performed. However, tumor margins in one of our patients were inadequate and the patient underwent subsequent wide resection. Tumors are often removed piecemeal by surgical procedures, with curative wide resection considered to be the adequate treatment of choice [1].

Grossly, myxoinflammatory fibroblastic sarcoma forms a poorly circumscribed mass surrounding the tendon sheath that may extend into the dermis and skeletal muscle. Microscopically, the tumor is characterized by solid nests of atypical spindle and epithelioid cells in a myxoid stroma and dense inflammatory infiltrates. The tumor cells often have large vesicular nuclei similar to those of virocytes or Reed-Sternberg cells. The immunophenotype is positive for vimentin, with variable immunoreactivity for CD34, CD68, cytokeratin, and smooth-muscle actin [1–6].

On MR images, myxoinflammatory fibroblastic sarcoma typically manifests as a poorly circumscribed mass with a multinodular appearance. Extensive involvement surrounding the tendon sheath is also a common feature.

The appearance of the extension along the tendon sheath in this tumor is similar to that seen in tenosynovitis. Differentiating tenosynovitis from myxoinflammatory fibroblastic sarcoma solely on MRI findings is difficult. Tenosynovitis also can lead to an ill-defined soft-tissue mass or enlargement of its sheath. However, this condition typically manifests as the accumulation of fluid with increased signal intensity of the affected tendon on T2-weighted MR images [8]. Clinical characteristics can allow the differentiation of tenosynovitis from myxoinflammatory fibroblastic sarcoma because tenosynovitis often decreases in size during the course of disease, whereas myxoinflammatory fibroblastic sarcoma usually grows with infiltration [1].

MRI findings of myxoinflammatory fibroblastic sarcoma also closely resemble those of giant cell tumors of the tendon sheath, proliferative fasciitis, acral fibromyxoma, myxoid

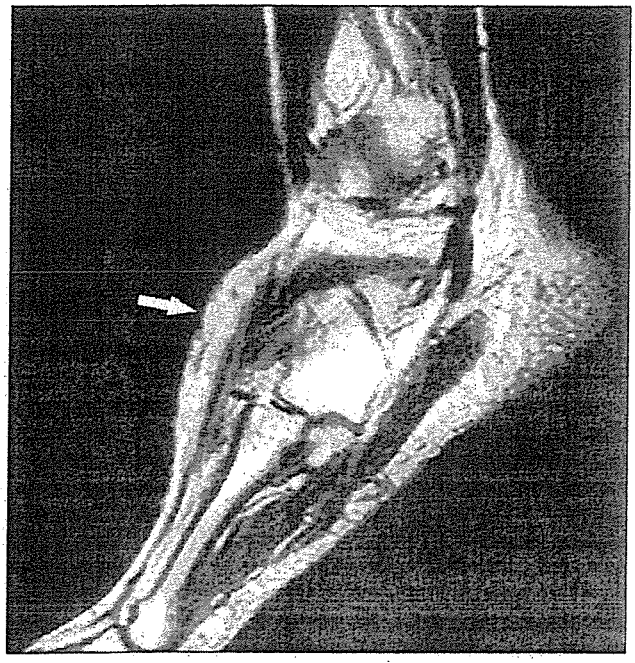

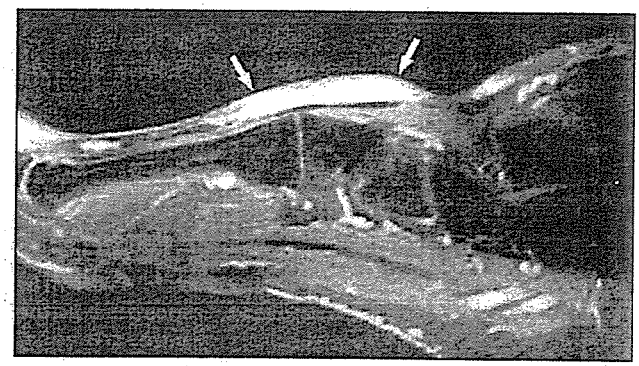

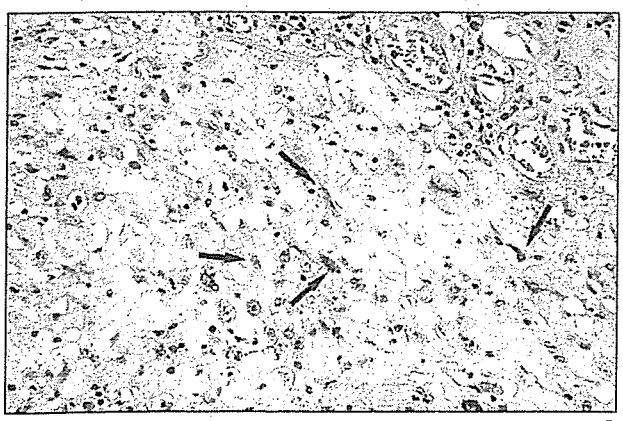

Fig. 3.—Myxoinflammatory fibroblastic sarcoma in foot of 32-year-old woman with local recurrence.
A, Sagittal T2-weighted MR image (TR/TE, 3,600/120) shows mass of sheetlike appearance beneath dorsal portion of tendon sheath. Tumor shows intermediate signal intensity, greater than that of muscle (*arrow*).
B, Sagittal contrast-enhanced fat-saturated T1-weighted MR image (520/15) shows homogeneous enhancement of tumor (*arrows*).
C, Photograph of histopathologic specimen shows sheetlike proliferation of spindle-shaped tumor cells (*arrows*) with ganglionlike cells, Reed-Sternberg-like cells, and lymphoid cells surrounding tendon sheaths.

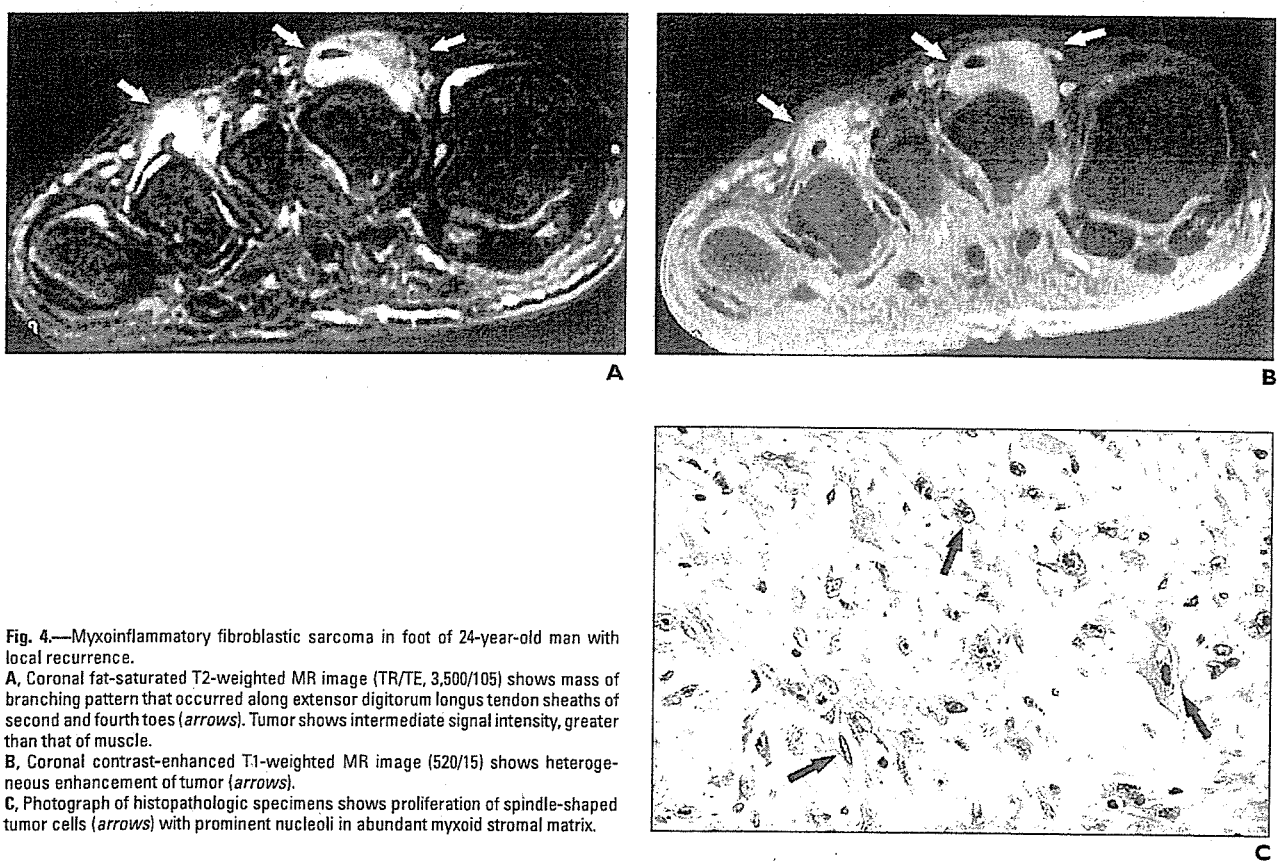

Fig. 4.—Myxoinflammatory fibroblastic sarcoma in foot of 24-year-old man with local recurrence.
A, Coronal fat-saturated T2-weighted MR image (TR/TE, 3,500/105) shows mass of branching pattern that occurred along extensor digitorum longus tendon sheaths of second and fourth toes (*arrows*). Tumor shows intermediate signal intensity, greater than that of muscle.
B, Coronal contrast-enhanced T1-weighted MR image (520/15) shows heterogeneous enhancement of tumor (*arrows*).
C, Photograph of histopathologic specimens shows proliferation of spindle-shaped tumor cells (*arrows*) with prominent nucleoli in abundant myxoid stromal matrix.

liposarcoma, and myxofibrosarcoma [9–13]. These conditions could not be distinguished radiologically from myxoinflammatory fibroblastic sarcoma on the basis of our study results. Signal characteristics and enhancement patterns were nonspecific. However, heterogeneous enhancement on contrast-enhanced MR images corresponded to geographic areas of the myxoid stromal matrix in the pathologic specimens. In two of our patients, MRI findings of recurrent tumors were ill defined and the tumors had sheetlike appearances involving the tendon sheath. A significant association may exist between recurrent tumors and the tendon sheath.

In summary, myxoinflammatory fibroblastic sarcoma typically affects adult subjects as a painless mass of the distal extremities at presentation. Myxoinflammatory fibroblastic sarcoma usually manifests on MR images as a multinodular and poorly circumscribed mass involving the surrounding tendon sheath. Although it is unlikely that such a rare condition could reasonably be diagnosed on the basis of MRI findings alone, the condition should be considered in the differential diagnosis of a soft-tissue mass in the distal extremities of adult patients.

References

1. Meis-Kindblom JM, Kindblom LG. Acral myxoinflammatory fibroblastic sarcoma: a low-grade tumor of the hands and feet. *Am J Surg Pathol* 1998;22:911–924
2. Montgomery EA, Devaney KO, Giordano TJ, Weiss SW. Inflammatory myxohyaline tumor of distal extremities with virocyte or Reed-Sternberg-like cells: a distinctive lesion with features simulating inflammatory conditions, Hodgkin's disease, and various sarcomas. *Mod Pathol* 1998;11:384–391
3. Lambert I, Debiec-Rychter M, Guelinckx P, Hagemeijer A, Sciot R. Acral myxoinflammatory fibroblastic sarcoma with unique clonal chromosomal changes. *Virchows Arch* 2001;438:509–512
4. Jurcic V, Zidar A, Montiel MD, et al. Myxoinflammatory fibroblastic sarcoma: a tumor not restricted to acral sites. *Ann Diagn Pathol* 2002;6:272–280
5. Sakaki M, Hirokawa M, Wakatsuki S, et al. Acral myxoinflammatory fibroblastic sarcoma: a report of five cases and review of the literature. *Virchows Arch* 2003;442:25–30
6. Pohar-Marinsek Z, Flezar M, Lamovec J. Acral myxoinflammatory fibroblastic sarcoma in FNAB samples: can we distinguish it from other myxoid lesions? *Cytopathology* 2003;14:73–78
7. Weiss SW, Goldblum JR. *Enzinger and Weiss's soft tissue tumors*, 4th ed. St. Louis, MO: Mosby, 2001:1552–1571
8. Mallefert JF, Dardel P, Cherasse A, Mistrih R, Krause D, Tavernier C. Magnetic resonance imaging in the assessment of synovial inflammation of the hindfoot in patients with rheumatoid arthritis and other polyarthritis. *Eur J Radiol* 2003;47:1–5
9. Llauger J, Palmer J, Monill JM, Franquet T, Bague S, Roson N. MR imaging of benign soft-tissue masses of the foot and ankle. *RadioGraphics* 1998;18:1481–1498
10. Kato K, Ehara S, Nishida J, Satoh T. Rapid involution of proliferative fasciitis. *Skeletal Radiol* 2004;33:300–302
11. Fetsch JF, Laskin WB, Miettinen M. Superficial acral fibromyxoma: a clinicopathologic and immunohistochemical analysis of 37 cases of a distinctive soft tissue tumor with a predilection for the fingers and toes. *Hum Pathol* 2001;32:704–714
12. Tateishi U, Hasegawa T, Beppu Y, Kawai A, Satake M, Moriyama N. Prognostic significance of MRI findings in patients with myxoid-round cell liposarcoma. *AJR* 2004;182:725–731
13. Munk PL, Sallomi DF, Janzen DL, et al. Malignant fibrous histiocytoma of soft tissue imaging with emphasis on MRI. *J Comput Assist Tomogr* 1998;22:819–826

Reprint from

M. Kaminishi, K. Takubo, K. Mafune (Eds.)
The Diversity of Gastric Carcinoma
Pathogenesis, Diagnosis, and Therapy

Recent Advances in Radiology for the Diagnosis of Gastric Carcinoma

Gen Iinuma[1], Hideto Tomimatsu[1], Yukio Muramatsu[1], Noriyuki Moriyama[1], Toshiaki Kobayashi[2], Hiroshi Saito[2], Tetsuo Maeda[3], Kunihisa Miyakawa[3], Fumihiko Wakao[3], Mitsuo Satake[3], and Yasuaki Arai[3]

Introduction

Radiographic diagnosis of gastric carcinoma [1] was first introduced in the 1960s in Japan, which led the world in the early diagnosis of gastric carcinoma by double-contrast method using film-screen systems (FSS) [2,3]. Qualitative diagnostics, including diagnosis of the depth of tumor invasion, were explored thoroughly in the 1970s, and it could be claimed that the radiographic diagnosis of gastric carcinoma was completely established by the beginning of the 1980s [4]. Gastric radiography has now become a standard examination modality in the screening and preoperative staging of gastric carcinoma and is widely used across the globe. The mortality rate from gastric carcinoma is especially high in Japan, and gastric radiography has made a substantial contribution to the detection of gastric carcinoma in mass screening. With recent advances in endoscopic techniques, the primary role in the diagnosis of gastric carcinoma, including its early diagnosis, has been inherited by endoscopy, but it is also a fact that radiography is still widely used in clinical diagnosis in screening and preoperative staging [5]. The demand for computerization of medical information grew in the 1980s, and against a background of advances in image engineering, the digitalization of medical images has proceeded apace [6,7]. In gastric radiography, too, digitalization via digital radiography (DR) using high-resolution charge-coupled device (CCD) cameras (CCD-DR) has been established and disseminated rapidly, and we also have reported its usefulness in the diagnosis of gastric carcinoma [8]. Meanwhile, a recent major development in the field of radiology has been the emergence of multidetector row computed tomography (CT) (MDCT) [9]. With the advent of MDCT in the second half of the 1990s, CT has achieved increased efficiencies and improved image quality in a revolutionary scanning modality [10]. In the preoperative staging of gastric carcinoma, it is now possible to accurately evaluate local inva-

[1]Cancer Screening Division, Research Center for Cancer Prevention and Screening, [2]Cancer Screening Technology Division, Research Center for Cancer Prevention and Screening, [3]Diagnostic Radiology Division, National Cancer Center Hospital, National Cancer Center, 5-1-1 Tsukiji, Chuo-ku, Tokyo 104-0045, Japan
e-mail: giinuma@gan2.ncc.go.jp

sion and small metastases, and three-dimensional (3D) MDCT imaging (MDCT gastrography) has arrived on the scene as a new diagnostic tool for primary lesions.

In this chapter, we describe the present status of radiologic diagnosis of gastric carcinoma using CCD-DR at our center, report our experience of MDCT gastrography in the preoperative staging of gastric carcinoma, and discuss the future prospects for radiographic diagnosis of gastric carcinoma using these new diagnostic techniques.

Advanced Digital Radiographic Systems for Gastric Diagnosis

In our hospital, images yielded by radiography of the gastrointestinal tract became completely digitalized with the adoption of CCD-DR (DR-2000H; Hitachi Medical, Tokyo, Japan) in 1999. At present, hard copies of diagnostic images are prepared for interpretation, but monitor-based diagnosis is yet to become a reality. Our radiographic investigations of the gastrointestinal tract use three CCD-DR systems: one C-arm type, one over-tube type, and one under-tube type. Each CCD-DR is connected by a DR network to two laser printers and an image server, and in parallel with the scanning procedure, reference images are forwarded to the hospital information system via a gateway after DICOM (digital imaging and communication in medicine) conversion at the same time as the diagnostic images are processed. After DICOM

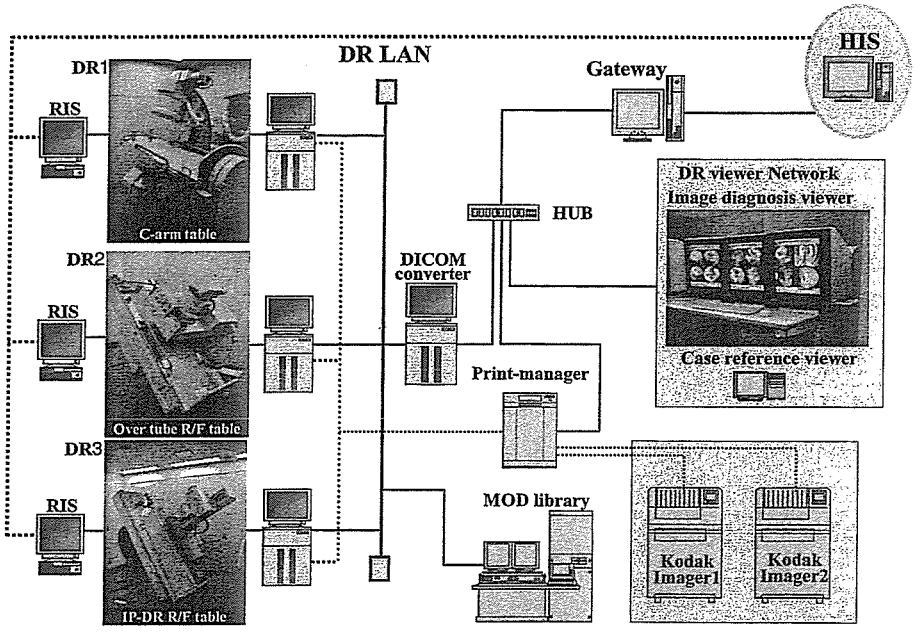

FIG. 1. Advanced digital radiography system for gastric diagnosis. Three charge-coupled device-digital radiography (CCD-DR) units are routinely used for gastric examinations in our hospital. Each unit connects with a DR network, and the images can be diagnosed on an image workstation

conversion, the images are accessible for monitor diagnosis at an image workstation with three viewers (Fig. 1).

The Status of CCD-DR-Based Radiographic Examination of Gastric Carcinoma

At our center, we use 250–300 ml barium at a 130–140 w/v% concentration in gastric radiographic studies. The scanning methods employed are the filling method, double-contrast radiography, and the compression method, but the core diagnostic technique in radiographic diagnosis of gastric carcinoma is double-contrast imaging obtained with barium (positive contrast medium) and gas (negative contrast medium). After barium is swallowed, the patient is given 5 g of a foaming agent, and by distending the stomach via the CO_2 gas so produced, we are able to easily obtain double-contrast images. The barium contained in the gas-distended stomach moves with changes in posture, and double-contrast images of excellent quality are obtained by ensuring that the barium adheres uniformly to the mucosal surfaces. Unlike the filling and compression methods, double-contrast imaging is indispensable for the visualization of early gastric carcinoma, which is characterized by few irregularities of the mucosal surfaces (Fig. 2). With gastric radiography based on the double-contrast method, we can easily identify the macroscopic types of gastric carcinomas, their exact extensions and locations in the stomach (Figs. 3–6). However, viewing double-contrast images obtained with contrast provided by gas and barium requires a broad dynamic range. The dynamic range for CCD-DR images adequately covers the image quality required for gastric radiography, and the image quality matches that in conventional FSS. Additionally, CCD-DR digital images also enable the optimization of image quality via image processing after scanning and, compared with FSS, are relatively well matched image by image and allow standardized diagnostic images to be obtained.

Comparative Evaluation of FSS and CCD-DR in the Diagnosis of Gastric Carcinoma

We conducted a prospective study to evaluate the difference in diagnostic accuracy between FSS and CCD-DR, and reported in a publication of *Radiology* [8]. From January to February 1997, we randomly assigned patients scheduled for gastric radiography to either FSS or CCD-DR; 112 patients were examined by FSS and 113 by CCD-DR. Six radiologists who were blinded to the clinical details assessed the films for each patient with a six-level confidence rating for the presence or absence of gastric carcinoma. The CCD-DR images in this study were prepared as hard copies for diagnosis. The diagnoses for each patient were rated against those produced by three other radiologists who conducted the actual radiographic examinations and were aware of all clinical data, such as endoscopic findings and the pathology of biopsy specimens. The sensitivity and specificity of FSS and CCD-DR for gastric carcinoma were determined from the assessments obtained, the difference between the two modalities was statistically analyzed, and a comparison was performed by receiver-operating characteristic (ROC) analysis. The study yielded a diagnosis of gastric carcinoma by FSS in 24 patients and by CCD-DR in 27 patients; the sensitivity for diagnosing the presence of gastric carcinoma was 64.6% and 75.3%, respectively

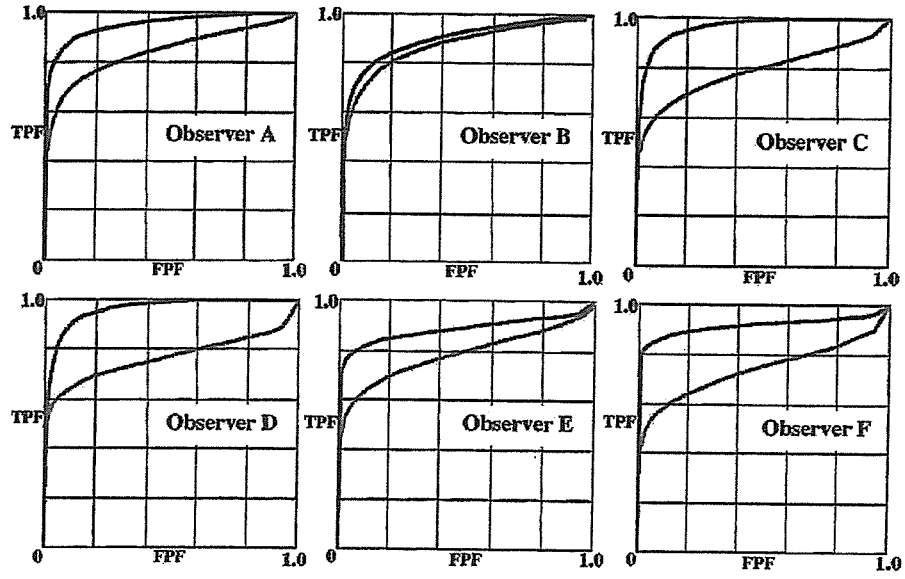

FIG. 7. Receiver operating characteristic (ROC) curves obtained from six observers. All observers achieved more accurate results with CCD-DR than with conventional radiography. Diagnostic accuracy of CCD-DR is clearly superior to that of conventional radiography. (Used with permission from Radiological Society of North America)

($P = 0.278$), and the specificity was 84.5% and 90.5%, respectively ($P = 0.011$). The ROC analysis [11] also showed that the diagnostic performance of CCD-DR was clearly superior (Fig. 7).

Usefulness of Radiography of Gastric Carcinoma by CCD-DR

The diagnostic performance of CCD-DR for gastric carcinoma is adequately comparable to that of FSS, indicating that the digitalization of images in gastric radiography is entirely feasible. The future adoption of diagnosis by monitor display will make possible the real-time display and optimization of diagnostic images and enable greater ease of image storage and retrieval. Capitalizing on these advantages of digitalization promises to yield an efficient and effective diagnostic environment for screening and preoperative staging, as compared with the conventional FSS modality.

Preoperative Evaluation of Gastric Carcinoma Using MDCT

To date, the role of radiographic CT studies in the preoperative staging of gastric carcinoma has primarily involved evaluating invasion of surrounding organs or metastasis to lymph nodes or other organs, and it was rare for it to be used for evaluation of the primary tumor itself [12,13]. However, the advent of MDCT has made possible the arrival of full-scale volume scans, facilitating high-speed, detailed image acquisition over an extensive area. The degree of resolution of CT images has improved

dramatically with MDCT, enabling the detailed evaluation of local lesions and the detection of small metastases, even in ordinary axial images [14]. Moreover, workstations that are capable of processing the massive quantities of image data produced by MDCT have been developed, and the three-dimensional CT visualization of gastric lesions, which is called MDCT gastrography, has become straightforward. This trend is fairly flourishing in the diagnosis of colorectal cancer as MDCT colonography, which is considered to have a great potential of being a modality for colorectal cancer screening [15–17].

Three-Dimensional Visualization of the Stomach by MDCT Gastrography

To visualize gastric lesions in three dimensions using MDCT, it is necessary to distend the gastric lumen with a foaming agent (CO_2 gas). As a consequence of the contrast between the gas and the inner gastric surface, owing to the substantial difference in density, it is possible to effortlessly prepare 3D images of the inner gastric surface. MDCT gastrography employs two methods for visualization, virtual endoscopic views and 3D gas insufflation views, obtained by 3D processing of the CT image data (Fig. 8).

Evaluation of the Detectability of Gastric Carcinoma by MDCT Gastrography

In the 3-month period between March and June 2003, we evaluated 4-row MDCT (Aquilion; Toshiba Medical Systems, Tokyo, Japan) in 84 gastric carcinoma patients who underwent MDCT for preoperative staging. Each scan was performed with the standard abdominal scan parameter settings for preoperative staging using automatic exposure control [18]. We prepared virtual endoscopic and 3D gas insufflation views from the image data obtained for each patient by MDCT volume scans, and two radiologists prepared responses on the basis of all clinical data for each patient, including gastroscopic findings, and the detectability of gastric carcinoma was evaluated by consensus for each display method. Eighty-six gastric carcinoma lesions (44 early and 42 advanced lesions) were diagnosed in the 84 patients. The detectability by virtual endoscopic and 3D gas insufflation views by MDCT gastrography was 47.7% and 40.9%, respectively, for early lesions (Table 1), and 59.5% and 76.2% for advanced lesions (Table 2). Hence, the detectability was less than 50% for early lesions, but about 60%–70% for advanced lesions of gastric carcinoma [19]. Especially in early lesions, all protruded-type lesions could be recognized, while less than half of depressed-type lesions, which is a common type of early gastric carcinoma, were missed (Figs. 9, 10).

TABLE 1. Detectability for 44 early gastric carcinomas by multidetector row computed tomography (MDCT) gastrography

	Protruded type	Flat elevated type	Depressed type	Total
Virtual endoscopic views	100% (2/2)	50.0% (1/2)	45.0% (18/40)	47.7% (21/44)
Three-dimensional gas insufflation views	100% (2/2)	50.0% (1/2)	37.5% (15/40)	40.9% (18/44)

TABLE 2. Detectability for 42 advanced gastric cancers by MDCT gastrography

	Borrman I type	Borrman II type	Borrman III type	Borrman IV type	Total
Virtual endoscopic view	0% (0/1)	84.6% (11/13)	68.8% (11/16)	25.0% (3/12)	59.5% (25/42)
Three-dimensional gas insufflation view	0% (0/1)	76.9% (10/13)	68.8% (11/16)	91.7% (11/12)	76.2% (32/42)

MDCT gastrography is presently inadequate for the detection of gastric carcinoma and its potential for clinical application is low.

Potential for MDCT Gastrography in Preoperative Staging for Gastric Carcinoma

MDCT gastrography is simpler and less invasive than endoscopy and radiography, and permits evaluation of the stomach overall in an examination of short duration. Detection of early lesions is challenging, and although it therefore has low potential as a screening method, it is capable of detecting lesions that are advanced to a certain extent, and also of simultaneously detecting lesions in other organs of the abdomen. In preoperative staging, as for radiography, it is capable of objectively ascertaining the position and overall picture of the primary lesion, and of diagnosing the relations between the degree of extramural invasion and surrounding organs. With the axial images of MDCT, representing a quantum leap in resolution compared with normal CT, it was possible to also diagnose correctly lymph node metastasis. Because MDCT itself is an examination method required for the preoperative diagnosis of local spread or remote metastasis of gastric carcinoma, it is highly likely at present that it can partially replace the role of radiography or ultrasound endoscopy. As well, because the image data of MDCT is digitalized density information, it is possible to selectively visualize 3D information in a manner that is effective for diagnosis, and has a great potential of being a modality for computer-aided diagnosis [20]. By digitally combining the 3D view of the primary lesion and the 3D image data of diagnosed lymph node metastasis, it will be possible to provide surgeons with effective preoperative 3D views of gastric carcinoma (Fig. 11).

Conclusions

As a result of future advancements in image engineering and computer technology, digital radiographic systems and MDCT systems will continue to evolve, and it can be predicted that new diagnostic methods that utilize the advantages of digitalization in the radiological diagnosis of gastric carcinoma will also be developed. MDCT gastrography has little potential at present as a diagnostic method for the primary lesions of gastric carcinoma. However, with further advances in MDCT, higher-speed examinations, improved image quality, and optimization of exposure dose, it appears certain that MDCT gastrography will gradually replace radiography, endoscopy, and ultrasound endoscopy.

Acknowledgments. This work was supported by Grants for Scientific Research Expenses for Health and Welfare Programs and the Foundation for the Promotion of Cancer Research, and by the 3rd-term Comprehensive 10-year Strategy for Cancer Control from the Ministry of Health, Labor and Welfare.

References

1. Templeton FE (1964) X-ray examination of the stomach, rev edn. University of Chicago Press, Chicago
2. Kuru M (1966) X-ray diagnosis. In: Atlas of early gastric carcinoma of the stomach. Nakayama-Shoten, Tokyo, pp 219–223
3. Shirakabe H, Ichikwa H, Kumakura K, et al (1966) Atlas of X-ray diagnosis of early gastric cancer. Igaku Shoin, Tokyo
4. Ichikawa H (1993) X-ray diagnosis of early gastric cancer. Gastric cancer. Springer-Verlag, Tokyo, pp 232–245
5. Okumura T, Maruyama M (1993) A prospective study on advanced gastric cancer detection by mass screening. Gastric Cancer. Springer-Verlag, Tokyo, pp 263–277
6. Sonoda M, Takano M, Miyahara J, et al (1983) Computed radiography utilizing scanning laser stimulated luminescence. Radiology 148:833–838
7. Hillman BJ, Ovitt TW, Nudelman S, et al (1981) Digital video subtraction angiography of renal vascular abnormalities. Radiology 139:277–280
8. Iinuma G, Ushio K, Ishikawa T, et al (2001) Diagnosis of gastric cancers: comparison of conventional radiography with a 4 million-pixels charge-coupled device. Radiology 214: 497–502
9. Berland LL, Smith JK (1998) Multidetector-array CT: once again, technology creates new opportunities. Radiology 209:327–329
10. Hu H, He HD, Foley WD, Fox SH (2000) Four multidetector-row helical CT: image quality and volume coverage speed. Radiology 215:55–62
11. Metz CE, Goodenough DJ, Rossmann K (1973) Evaluation of receiver operating characteristic curve data in terms of information theory, with applications in radiography. Radiology 109:297–303
12. Botet JF, Lightdale CJ, Zauber AG, et al (1991) Preoperative staging of gastric cancer: comparison of endoscopic US and dynamic CT. Radiology 181:426–432
13. Habermann RC, Weiss F, Riecken R, et al (2004) Preoperative staging of gastric adenocarcinoma: comparison of helical CT and endoscopic US. Radiology 230:465–471
14. Ba-Ssalamah A, Prokop M, Uffmann M, et al (2003) Dedicated multidetector CT of the stomach: spectrum of diseases. *Radiographics* 181:426–432
15. Dachman A (2003) Atlas of virtual colonoscopy. Springer-Verlag, New York
16. Iannaccone R, Laghi A, Catalano C, et al (2003) Detection of colorectal lesions: lower-dose multi-detector row helical CT colonography compared with conventional colonoscopy. Radiology 229:775–781
17. Macari M, Bini EJ, Jacobs SL, et al (2004) Colorectal polyps and cancers in asymptomatic average-risk patients: evaluation with CT colonography. Radiology 230:629–636
18. Itoh S, Ikeda M, Mori Y, et al (2002) Lung: feasibility of a method for changing tube current during low-dose helical CT. Radiology 224:905–912
19. Iinuma G, Moriyama N (2004) Clinical potential of CT gastrography for visualization of gastric cancers. In: Recent advances in gastric cancers: the 17th International Symposium of Foundation for Promotion of Cancer Research, pp 37–38
20. Summers RM (2003) Road maps for advancement of radiologic computer-aided detection in the 21st century. *Radiology* 229:11–13

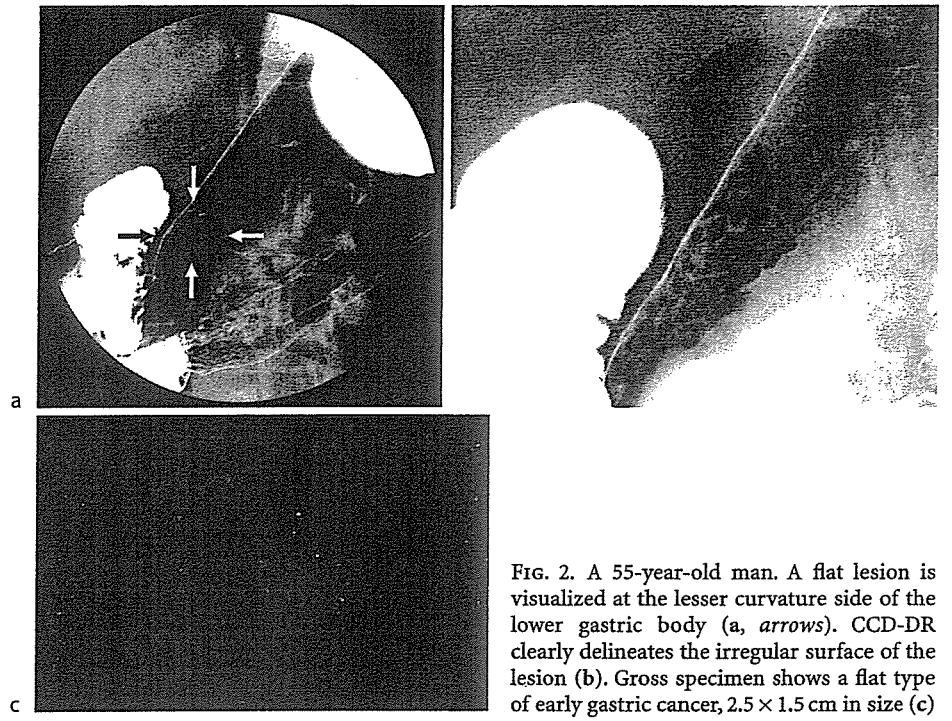

FIG. 2. A 55-year-old man. A flat lesion is visualized at the lesser curvature side of the lower gastric body (a, *arrows*). CCD-DR clearly delineates the irregular surface of the lesion (b). Gross specimen shows a flat type of early gastric cancer, 2.5 × 1.5 cm in size (c)

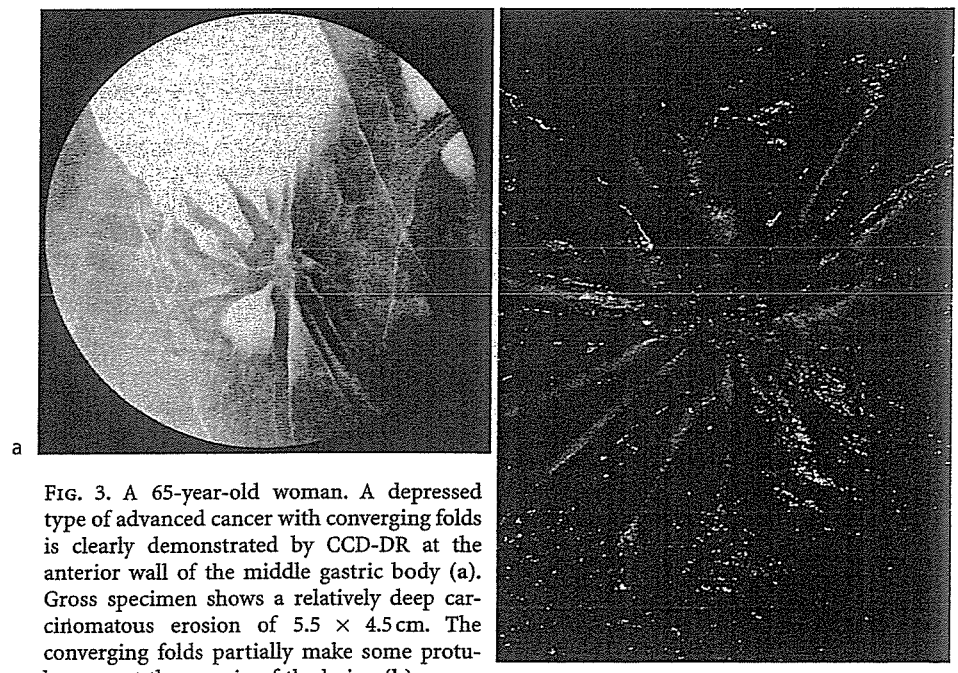

FIG. 3. A 65-year-old woman. A depressed type of advanced cancer with converging folds is clearly demonstrated by CCD-DR at the anterior wall of the middle gastric body (a). Gross specimen shows a relatively deep carcinomatous erosion of 5.5 × 4.5 cm. The converging folds partially make some protuberance at the margin of the lesion (b)

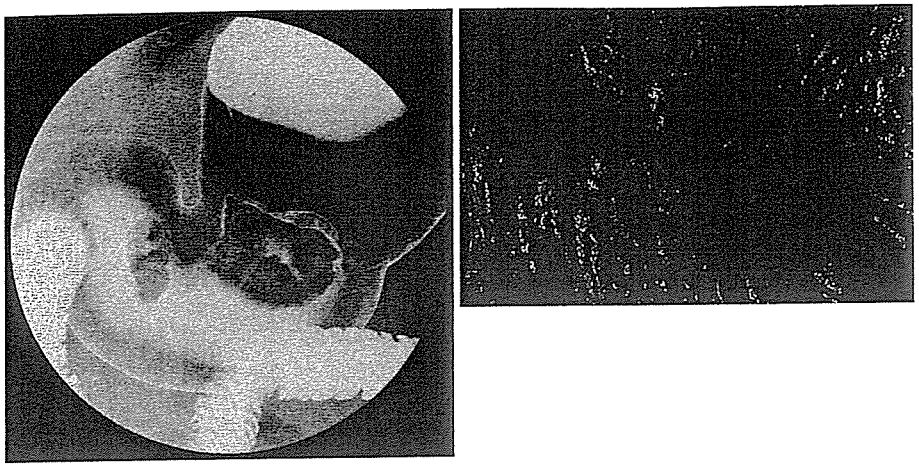

a b

FIG. 4. A 70-year-old man. CCD-DR visualizes two gastric cancers at the posterior of the lower gastric body to the antrum (a). Gross specimen demonstrates a protruded advanced cancer with central ulceration measuring 4.0 cm and a protruded type of early cancer measuring 2.0 cm (b)

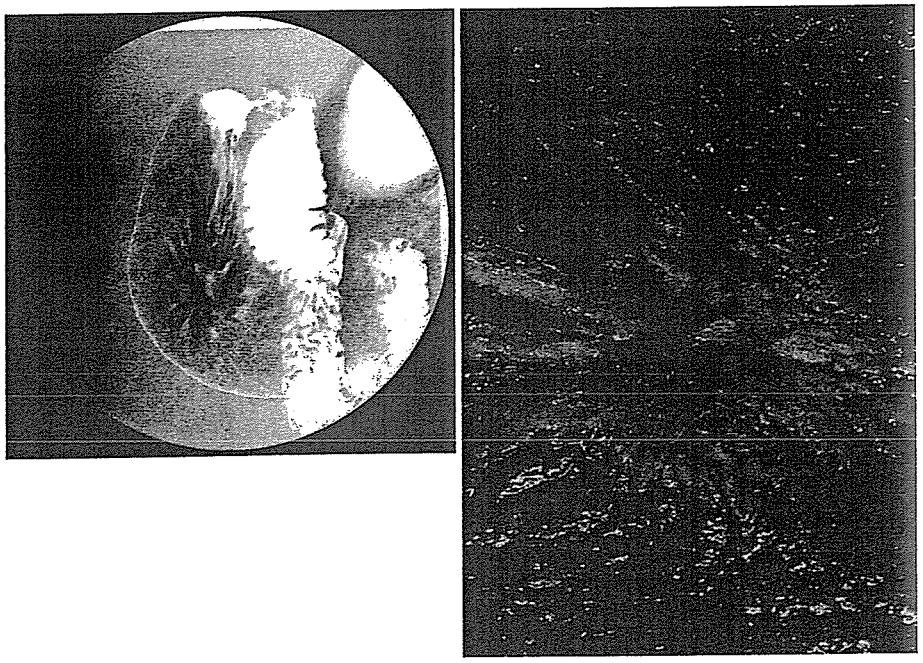

a b

FIG. 5. A 55-year-old man. CCD-DR demonstrates a depressed type of gastric cancer at the posterior wall of the antrum (a). Gross specimen shows a depressed type of advanced cancer 5.0 × 4.5 cm in size (b)